NASA Contractor Report 178018

ICASE REPORT NO. 85-52

ICASE

ACTIVE CONTROL OF COMPRESSIBLE FLOWS ON A CURVED SURFACE

Lucio Maestrello
Paresh Parikh
Alvin Bayliss
Eli Turkel

Contracts No. NAS1-17070 and NAS1-18107
November 1985

INSTITUTE FOR COMPUTER APPLICATIONS IN SCIENCE AND ENGINEERING
NASA Langley Research Center, Hampton, Virginia 23665

Operated by the Universities Space Research Association

National Aeronautics and
Space Administration

Langley Research Center
Hampton, Virginia 23665

7 1 1 UTP/ACTIVE *+1 CONTROL *+2 COMPRESSIBLE *+1 F
DISPLAY 07/6/1
86N18648*# ISSUE 9 PAGE 1424 CATEGORY 34 RPT*: NASA-CR-178018
ICASE-85-52 NAS 1.26:178018 CNT*: NAS1-17070 NAS1-18107 NAS1-17252
85/11/00 29 PAGES UNCLASSIFIED DOCUMENT

UTTL: Active control of compressible flows on a curved surface TLSP: Final Report

AUTH: A/MAESTRELLO, L.; B/PARIKH, P.; C/BAVLISS, A.; D/TURKEL, E. PAA: B/(Vigyan Research Associates, Inc., Hampton, Va.); C/(Exxon Corporate Research Science Labs.); D/(Tel-Aviv Univ., Israel)

CORP: National Aeronautics and Space Administration. Langley Research Center, Hampton, Va. AVAIL.NTIS

SAP: HC A02/MF A01

CIO: UNITED STATES

MAJS: /*ACTIVE CONTROL/*COMPRESSIBLE FLOW/*CONTOURS/*HEATING/*SOLID SURFACES/* SURFACE COOLING

MINS: / NAVIER-STOKES EQUATION/ PRESSURE GRADIENTS/ STEADY FLOW/ TURBULENCE EFFECTS/ WAVE PROPAGATION

ABA: Author

ACTIVE CONTROL OF COMPRESSIBLE FLOWS ON A CURVED SURFACE

Lucio Maestrello
NASA Langley Research Center

Paresh Parikh
Vigyan Research Associates, Inc.

Alvin Bayliss
Exxon Corporate Research Science Laboratories

Eli Turkel
Institte for Computer Applications in Science and Engineering
and
Tel-Aviv University, Tel-Aviv, Israel

ABSTRACT

We consider the effect of localized, time-periodic surface heating and cooling over a curved surface. This is a mechanism for the active control of unstable disturbances by phase cancellation and reinforcement. It is shown that the pressure gradient induced by the curvature significantly enhances the effectiveness of this form of active control. In particular, by appropriate choice of phase, active surface heating can completely stabilize an unstable wave.

Partial support for this research was provided for the second author under NASA Contract No. NAS1-17252.

Additional research was partially supported under NASA Contracts No. NAS1-17070 and NAS1-18107 while the third and fourth authors were in residence at the Institute for Computer Applications in Science and Engineering, NASA Langley Research Center, Hampton, VA 23665-5225.

1. INTRODUCTION

The effect of surface curvature on laminar-turbulent transition in compressible flows can be calculated from the Navier-Stokes equations. From both a theoretical and an experimental point of view, it is natural to inquire as to how transition is affected by a pressure gradient induced by surface curvature. The pressure gradient introduces a coupling of the mean flow with external disturbances (sound, vorticity or entropy disturbances) that is much stronger than in flows with zero pressure gradient (i.e., flows over a flat plate). This coupling, in turn, causes rapid changes in the boundary layer when outside disturbances have sufficient amplitude to trigger the instability. Put another way, the receptivity of the flow is significantly enhanced.

References [1,2] show direct experimental evidence of this.* Historically, these disturbances, interacting with the mean flow in regions of significant pressure gradient, have been the source of discrepancies in the transition Reynolds numbers that have been reported. The receptivity of flows has been systematically investigated recently [1,2] and used as a mechanism for boundary layer triggering and for transition control [3,5].

Receptivity in its full meaning refers to the effect of both steady and unsteady disturbances on a mean (i.e., steady) flow.** The use of unsteady disturbances to modify features of a flow field is called active control.

---

*See also Kozlov, V. V. and Levchenko, V. Ya: "Laminar-turbulent transition control by localized disturbances." Preprint.

** Nishioka, M. and Morkovin, M. V.: "Boundary-layer receptivity to unsteady pressure gradient: Experiments and overview," 1984.

Typically, active control techniques introduce unsteady disturbances to modify growing waves propagating through the flow. Active control can be used to cancel growing disturbances [5] or to trigger instabilities and instantaneous transition [3]. Active control can be effected by localized time periodic surface heating [5], or by introducing localized vibrations [7]. Active control by time-dependent surface cooling has not been accomplished but is at least theoretically possible at very low frequencies by using Peltier chips on the surface [8].

Specifically, it was shown in [5] that time-dependent, localized surface heating could be used to cancel growing disturbances in water. An analysis of the effect of surface heating in both water and air was presented in [3], [6]. In [7] vibrating ribbons were used to both cancel and amplify disturbances in air. In these experiments there was no surface curvature and thus little, if any, mean pressure gradient. On the other hand, it was shown in [3] that instantaneous transition in air could be achieved by heating near a leading edge where the pressure gradient is very large. No such effect was obtained when the flow was heated in regions where the surface was flat and the pressure gradient was weak.

A numerical simulation of the active control of unstable waves by localized, time-periodic surface heating and cooling in air was presented in [9,10]. These results are for compressible, subsonic flows over a flat plate so that there was no mean pressure gradient. The results demonstrated that both surface heating and cooling could be used to generate out of phase disturbances and cancel growing disturbances. In particular, active heating could be used to stabilize the flow, whereas steady heating of a flow over a flat plat is destabilizing. The amount of reduction of the amplitude of the

fluctuating disturbance was modest, although a larger reduction could be obtained by using multiple heating or cooling strips.

The objective of this paper is to study wave phenomena in a mean flow with a pressure gradient induced by surface curvature. The behavior of uncontrolled disturbances and the effect of active surface heating and cooling are studied. The numerical simulations are obtained by solving the compressible, two-dimensional Navier-Stokes equations over a curved surface.

Clearly, the inclusion of curvature permits a much wider range of features in the associated steady flow. The curvature can accelerate a subsonic flow into the transonic and supersonic regimes and shocks can develop. In particular, compressibility effects can be expected to become more important for accelerating flows with non-zero pressure gradient. In general, the enhanced receptivity of the mean flow due to the induced pressure gradient means that active surface heating and cooling would be expected to be considerably more effective than when applied over a flat plate. It will be shown that this is, in fact, the case.

The remainder of this paper is organized as follows. In section 2 the numerical scheme is discussed. In section 3 we present numerical results and in section 4 we summarize our conclusions.

2. NUMERICAL METHOD

We consider the compressible, two-dimensional Navier-Stokes equations. In Cartesian coordinates, x and y, these equations can be written in the conservation form

$$W_t = \tilde{F}_x + \tilde{G}_y. \tag{2.1}$$

In (2.1) W is the vector $(\rho, \rho u, \rho v, E)^T$, ρ is the density, u and v are the x and y velocities respectively, and E is the total energy. The functional forms of the flux functions $\tilde{F}$ and $\tilde{G}$ are standard and will not be reproduced here for brevity. The system (2.1) is supplemented by the equation of state for an ideal gas

$$p = \rho RT,$$

where p is the pressure, T the temperature, and R is the gas constant.

In order to deal with surface curvature we consider a general, non-orthogonal coordinate transformation

$$\begin{aligned} \xi &= \xi(x,y) \\ \eta &= \eta(x,y) \end{aligned} . \tag{2.2}$$

The wall is the curve $\eta = 0$. Applying the transformation (2.2), the system (2.1) can be transformed to the new system

$$(JW)_t = F_\xi + G_\eta . \tag{2.3}$$

In (2.3) J is the Jacobian

$$J = x_\xi y_\eta - x_\eta y_\xi$$

and the new flux functions F and G are given by

$$F = \tilde{F} y_\eta - \tilde{G} x_\eta \quad \text{and} \quad G = \tilde{G} x_\xi - \tilde{F} y_\xi .$$

The transformed system (2.3) is solved by an explicit finite difference scheme using a uniform (ξ,η) grid in the computational plane. The viscous stresses must be transformed to the new coordinate system. The precise form of the transformed system of equations is omitted for brevity. The use of the Navier-Stokes equations in a transformed coordinate system is a common technique for dealing with curved boundaries. A more detailed discussion can be found in [11,12]. If the equation of the wall is given as

$$y = f(x),$$

then the coordinate transformation is

$$\xi = x \tag{2.4a}$$

$$\eta = \frac{(y - f(x))}{(y_T - f(x))} y_T \tag{2.4b}$$

where y_T is the top of the computational domain. An additional exponential stretching is applied to (2.4b) to increase the grid resolution near $\eta = 0$ where large variations in the solution have to be resolved. The transformation (2.4) is not orthogonal near the wall; however, the types of curvature considered in this paper are not particularly severe and the transformation (2.4) has been found to be adequate.

The finite difference scheme is a modification of the MacCormack scheme making it fourth-order accurate on the convective terms. The scheme is second-order accurate in time and is second-order on the viscous terms for non-constant viscosity. The fourth-order accuracy is essential in order to:

a) prevent viscous-like truncation errors on the convective terms from artificially decreasing the effective Reynolds number of the computation, and b) prevent numerical dispersion and dissipation from altering the character of the waves which are computed in the mean flow.

The numerical scheme is described in detail in [13]. The discussion below will therefore be brief. The numerical scheme applied to the one-dimensional equation

$$u_t = F_x$$

consists of a predictor of the form

$$\bar{u}_i = u_i^N + \frac{\Delta t}{6\Delta x}\left(-7F_i + 8F_{i+1} - F_{i+2}\right) \tag{2.5a}$$

together with a corrector of the form

$$u_i^{N+1} = \frac{1}{2}\left(\bar{u}_i + u_i^N + \frac{\Delta t}{6\Delta x}\left(7\bar{F}_i - 8\bar{F}_{i-1} + \bar{F}_{i-2}\right)\right). \tag{2.5b}$$

In (2.5) the subscript i denotes the spatial grid point and the superscript N denotes the time level. The scheme (2.5) is alternated with an obvious symmetric variant.

Two-dimensional problems are treated by operator splitting. For example, if L_x denotes the solution operator symbolized by (2.5) for the equation

$$W_t = F_x,$$

and L_y denotes the similar operator for the equation

$$W_t = G_y,$$

then the solution to the equation

$$W_t = F_x + G_y$$

is obtained by

$$W^{N+2} = L_x L_y L_y L_x W^N. \tag{2.6}$$

The split scheme (2.6) preserves the second-order accuracy in time. We stress that in the applications the scheme described above is applied to the transformed system (2.3).

A typical computational domain is shown in figure 1. In practice, a steady solution is first computed for a given geometry. The computed steady flow is disturbed by specifying an inflow disturbance. The inflow data can be written as

$$W_{inflow} = W_{mean} + \varepsilon \text{ real part } \left(e^{i\omega t} H(y)\right) \tag{2.7}$$

where ω is the frequency and $H(y)$ is a solution of the Orr-Sommerfeld equation for the inflow profile (assuming a flat geometry). The profiles used here were obtained from a program developed at NASA Langley Research Center by J. R. Dagenhart. The parameter ε is used to adjust the strength of the inflow disturbance.

A detailed discussion of boundary conditions is given in [13] and the reader is referred to that reference for details. For subsonic flows (2.7) is

used to provide three conditions at inflow. Approximate radiation conditions are used at the outflow and at the upper boundaries. At the wall the temperature is specified and the pressure is obtained from a first-order extrapolation in the η direction. Surface heating and cooling are simulated by locally modifying the temperature at the wall.

3. RESULTS

In this section we discuss the numerical results over the curved and the flat region of the surface. The results reported here will be for a curved surface with a height of 0.02 ft. We are currently investigating more severely curved surfaces and will report those results at a later date. The inflow Mach number is $M_e = 0.7$ and the unit Reynolds number is 3×10^5. The steady state Mach number and pressure coefficient are shown in figure 2. Upstream the surface is flat and the pressure gradient zero. This is the inflow region. Downstream the initial curvature is concave then it reverses into a convex shape, and further downstream it returns to its original flat shape. The pressure gradient and the flow Mach number change over the curvature. The pressure coefficients, C_p, increases along the concave region as the Mach number decreases due to adverse pressure gradient. Downstream in the convex region C_p decreases as the Mach number increases reaching a constant over the flat portion of the surface.

The curved wall is defined by a fourth degree polynomial

$$y = ax^4 + bx^3 + cx^2 + dx + e \tag{3.1}$$

where the coefficients are determined so as to specify the maximum height at $x = 1.2$ ft. and to insure that the surface smoothly becomes flat at the inflow and at the maximum. A fluctuating disturbance is induced at the inflow with nondimensional frequency $F = \left((2\pi f\nu)/U_e^2\right)$ of 0.8×10^{-4}. (Here f is the frequency, ν the kinematic viscosity, and U_e the free stream velocity.) It is known that this frequency is linearly unstable for the Reynolds number used at the inflow.

In figure 3 we compare the growth rates for the inflow disturbance over the curved surface with the growth rates obtained from the same inflow but on a flat surface. The parameter ε is chosen so that the maximum inflow disturbance is 2% of the free stream. The growth rates are computed by computing the RMS $\sqrt{\overline{(\rho u - (\rho u)_{mean})^2}}$ and integrating this quantity in y and normalizing by the value at inflow. The integration is taken up to the point where the Orr-Sommerfeld perturbation goes through zero for the particular x location. Qualitatively similar results were obtained by choosing the maximum disturbance level or integrating up to the edge of the boundary layer.

It is apparent from the figure that in the flat case the disturbance grows and decays in a manner similar to what would be expected from linear theory. With curvature the growth is initially enhanced due to the unfavorable pressure gradient and then stabilized due to the favorable pressure gradient. Once the surface becomes flat the solution exhibits a strong growth. This is because at the beginning of the flat region the magnitude of the disturbance has become sufficiently large so that the growth and decay are not governed by linear theory. In [9,10] the authors observed

that disturbances which were sufficiently large would not decay in the stable region whereas smaller disturbances would follow the stability curve closely.

The effect of active control is investigated in two regions of the surface corresponding to adverse and favorable pressure gradient. Surface heating and cooling are accomplished by modifying the temperature boundary condition over a small strip ($\sim 10\%$ of the wavelength of the disturbance at inflow) on the surface. The formula is

$$\frac{T}{T_{ref}} = \frac{T_w}{T_{ref}} \pm \left(\alpha + \beta^2 \sin^2\left(\frac{\omega t}{2} + \phi\right)\right), \tag{3.2}$$

with the plus sign for the heating and minus sign for cooling. In (3.2) T_w is the temperature of the wall (520^oR) and T_{ref} is the reference temperature. The functional form of (3.2) models a D.C. current (α) and an A.C. current (β) with phase ϕ. A typical grid size for the calculation is 251×61.

The parameters for the heated case are $\alpha = 1$, $\beta = 2.76$ corresponding to a peak temperature of 1650^oR. For the cooled case the parameters are $\alpha = 0.77$, $\beta = 1.7$ with a minimum temperature of about 190^oR. In the heated case the maximum temperature corresponds to roughly three times the unheated wall temperature which is close to the temperature obtained in [4] using a tungsten wire. In the cooled case the parameters are chosen so that the temperature will stay in the range where Sutherland's law is valid for the viscosity as a function of the temperature. Such a periodic cooling is not attainable by experimental techniques available at the present time except for very low frequencies. There were no numerical instabilities due to the large temperature perturbation but the heating forced a reduction in the allowable time-step.

In figures 4-7 we present growth rates for four cases of active control. In figures 4 and 5 the flow is heated and cooled with a strip centered at $x = 0.3$ ft. where $C_p = 0.03$. In each case the heating and cooling is effected with two different phases ($\phi = 0^o$ and $\phi = 90^o$). In figures 6 and 7 the strip is placed at $x = 0.7$ ft. corresponding to $C_p = -0.015$. In all cases the growth rates are compared with the uncontrolled results.

The results in these figures demonstrate that the solution is very sensitive to the phase of the control heating and cooling. In particular, the phase of the heating can be chosen to reduce the disturbance level to the point where there is no growth over the flat portion of the surface. By changing the phase the overall growth can be significantly enhanced. The effect of cooling is less dramatic but still strongly dependent on the phase.

We have not investigated intermediate phases. For maximum control or amplification one needs to explore a range of phases between 0^o and 90^o. However, the results demonstrate:

(a) Heating can be used to either trigger or stabilize the flow via the mechanism of phase cancellation or amplification;

(b) Both active heating and cooling are considerably more effective than in the cases with no curvature reported in [9,10].

In figure 8 we plot the RMS of the fluctuating ρu as a function of the vertical coordinate η (defined by (2.4b)) at $x = 0.5$ ft. The results for heating with the two different phases and the uncontrolled case are shown. The heating strip was at $x = 0.3$ ft. It is apparent that the heating does not change the basic structure of the Orr-Sommerfeld profile. We stress that

the inflow profile was obtained from an incompressible stability code which did not account for the curvature. It can be seen that the spatial behavior of the disturbance accounting for compressibility and curvature is qualitatively similar to profiles obtained for incompressible flows over flat surfaces.

In figure 9 we present the same results at $x = 1.5$ ft. In this case the heated case with $\phi = 0^{o}$ is stabilized while the uncontrolled case and the heated case with $\phi = 90^{o}$ exhibit a nonlinear growth. All three profiles, however, are very similar except for the amplitude.

In figure 10 the time varying ρu fluctuation at the first grid point above the wall is plotted for the two heated cases (heating strip at $x = 0.3$ ft.) and for the uncontrolled case. The plots are for $x = 0.3$, 0.4, and 0.5 ft. A significant amount of distortion is evident near the heating strip. However, at $x = 0.5$ ft. there is little remnant of this distortion due to the heating strip. This is presumably due to diffusion of heat. The residual effects of the heating at $x = 0.5$ ft. are an amplitude change and a slight change of phase. Observe that the uncontrolled disturbance at $x = 0.5$ ft. exhibits clear nonlinear distortion. Nonlinear distortion is also evident for $\phi = 90^{o}$ but the solution for $\phi = 0^{o}$ for which cancellation seems to have occurred, is quite sinusoidal.

Finally, in figure 11 we plot the fluctuating ρu at selected locations across the boundary layer for $x = 0.5$ ft. At all locations the amplitude is larger for $\phi = 90^{o}$ and smaller for $\phi = 0^{o}$ as would be expected from the integrated data in figure 4. The thermal diffusion is sufficiently strong so that no distortion due to the heating strip is evident. There is, however, a marked effect on the amplitude and phase.

4. CONCLUSION

The results presented here for a single curved surface demonstrate the enhanced receptivity of a mean flow with a non-zero pressure gradient to active surface heating and cooling. This is particularly striking in view of the small size of the curved wall and the small amount of acceleration. This is because the curvature is large on the viscous length scale even though it is very small on the inviscid scale.

It is clear that phase cancellation and amplification and not just static heating and cooling contribute to the control that is demonstrated in figures 4-7. In particular, active surface heating appears to be a viable mechanism for flow control in the presence of a favorable pressure gradient. We are presently extending these results to cases with more severe curvature yielding larger acceleration of the mean flow velocity.

REFERENCES

[1] Kachanov, Yu S. and Levchenko, V. Ya: "The resonant interaction of disturbances at laminar-turbulent transition in a boundary layer," J. Fluid Mech., Vol. 138, 1984, pp. 209-247.

[2] Kachanov, Yu S., Kozlov, V. V., and Levchenko, V. Ya: "Nonlinear development of a wave in a boundary layer," Fluid Dynamics translated from Russian, Vol. 12, No. 1, January-February 1977, pp. 383-390.

[3] Maestrello, L.: "Active transition fixing and control of boundary layer in air," AIAA Paper No. 85-0564, March 1985.

[4] Wazzan, A. R. and Gazley, C., Jr.: "The combined effects of pressure gradient and heating on stability and transition of water boundary layers," Second Intl. Conference on Drag Reduction, University of Cambridge, published by BHRA Fluid Engineering E3-23-E3-40, 1977.

[5] Liepmann, H. W. and Nosenchuck, D. M.: "Active control of laminar-turbulent transition," J. Fluid Mech., Vol. 118, 1982, pp. 201-204.

[6] Maestrello, L. and Ting, L., "Analysis of active control by surface heating," AIAA J., Vol. 23, 1985, pp. 1038-1045.

[7] Thomas A. S. W.: "The control of boundary layer transition using a wave-superposition principle," J. Fluid Mech., Vol. 137, 1983, pp. 233-250.

[8] Kitter, C.: Introduction to Solid State Physics, John Wiley and Son, New York, 1976, Chapter 8.

[9] Bayliss, A., Maestrello, L., Parikh, P., and Turkel, E.: "Numerical simulation of boundary layer excitation by surface heating/cooling," AIAA Paper No. 85-0565, March 1985. Accepted for publication in AIAA J.

[10] Bayliss, A., Maestrello, L., Parikh, P., and Turkel, E.: "Wave phenomena in a high Reynolds number compressible boundary layer," ICASE/NASA Workshop on Stability of Time-Dependent and Spatially Varying Flows, August 19-20, 1985.

[11] Rudy, D. H.: "Navier-Stokes solutions for two-dimensional subsonic base flow," Southeastern Conference on Theoretical and Applied Mechanics, May 1984.

[12] Anderson, D. A., Tannehill, J., and Pletcher, R. H.: Computational Fluid Mechanics and Heat Transfer, Hemisphere Publishing Corporation, 1984.

[13] Bayliss, A., Parikh, P., Maestrello, L., and Turkel, E.: "A fourth-order scheme for the unsteady compressible Navier-Stokes equations," AIAA-85-1694, July 1985.

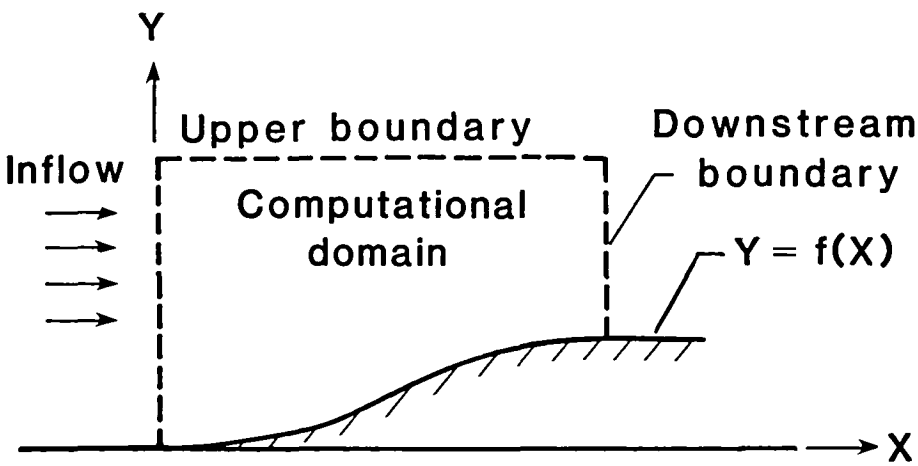

Fig. 1. Schematic of Computational Domain.

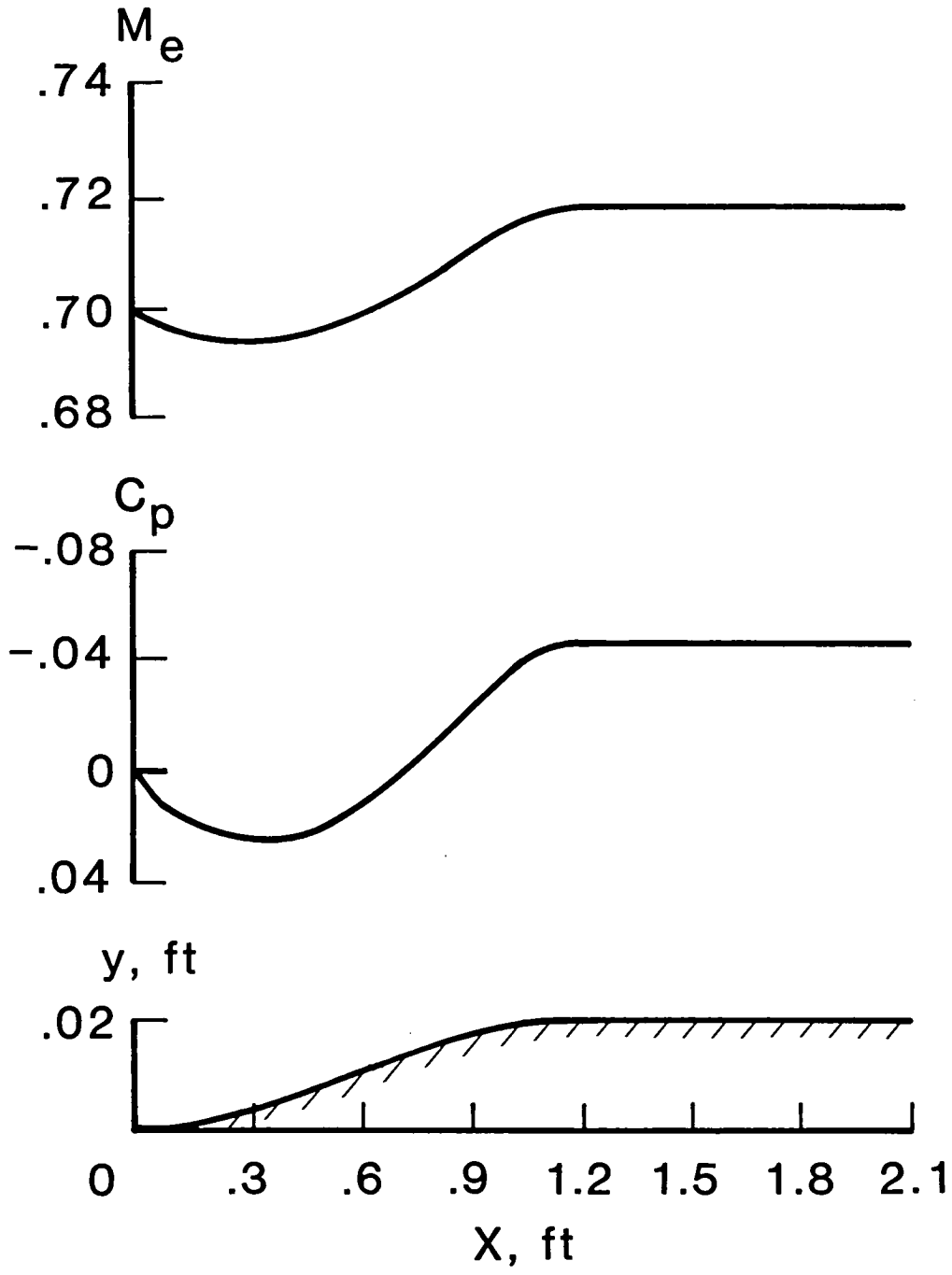

Fig. 2. Steady State Mach Number and Pressure Distribution on the Curved Surface.

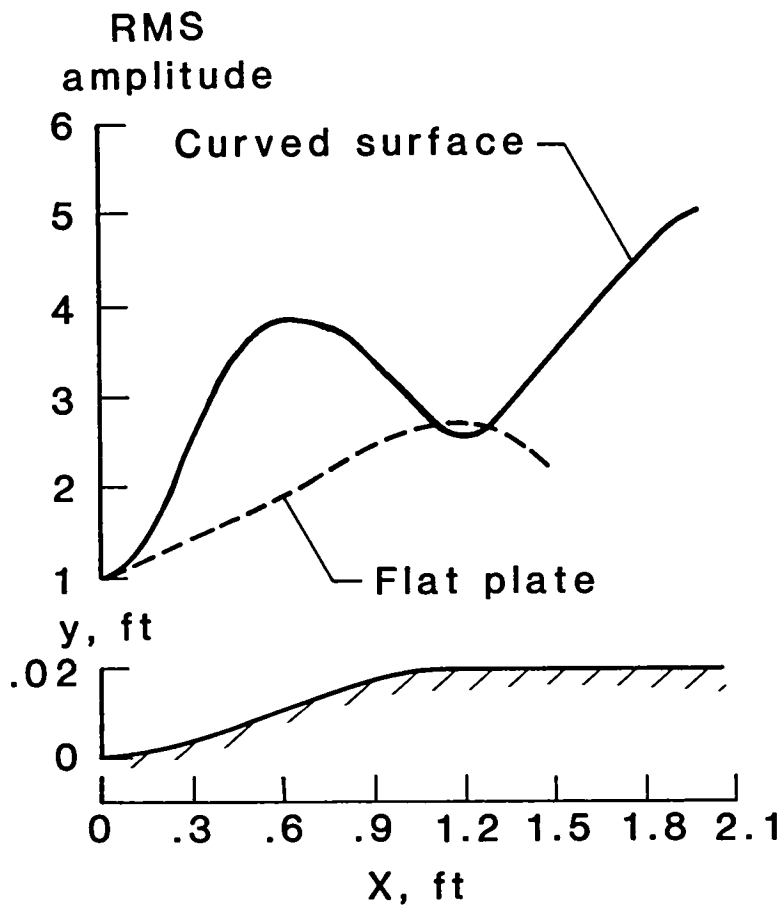

Fig. 3. Comparison of Growth Rates Between the Flat and the Curved Surface.

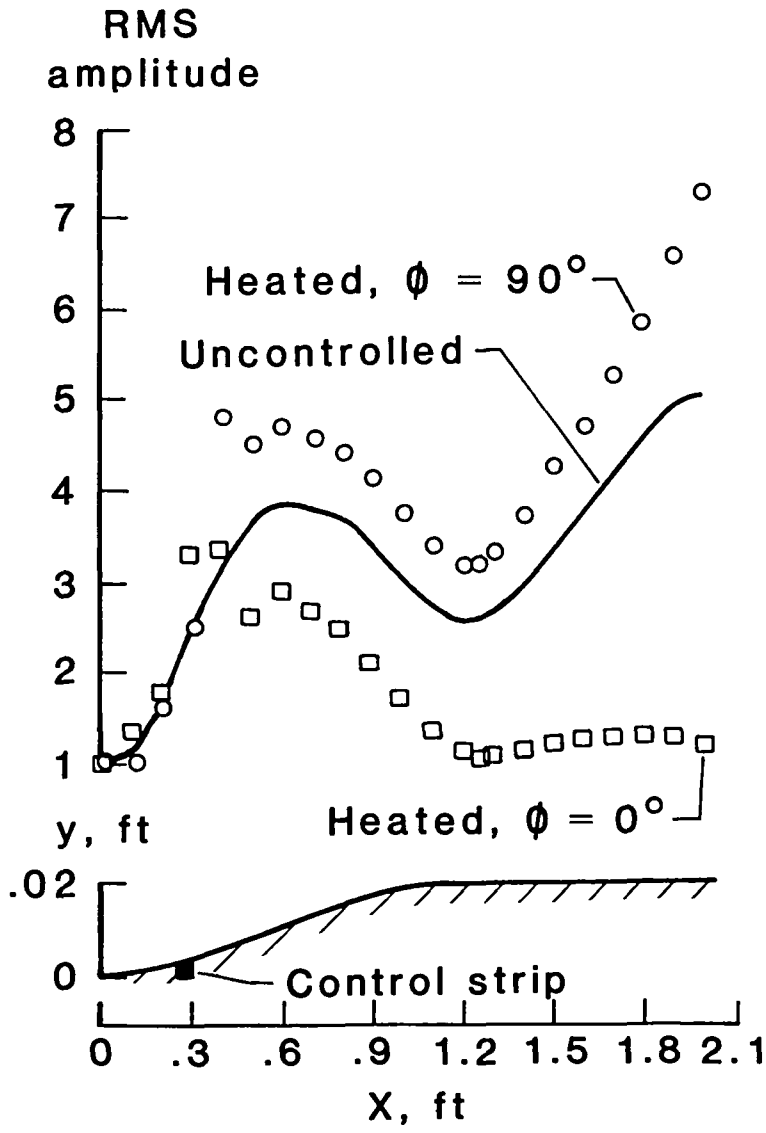

Fig. 4. Effectiveness of Active Control by Heating, Control Strip at x = 0.3 ft.

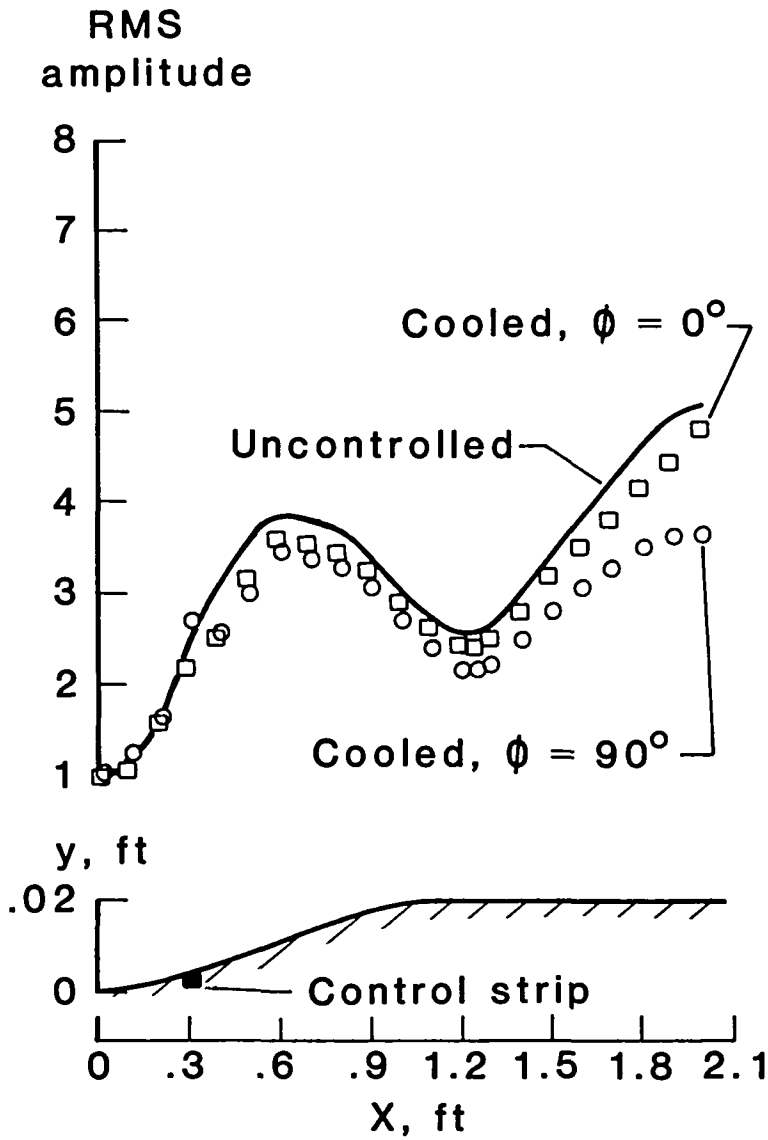

Fig. 5. Effectiveness of Active Control by Cooling, Control Strip at x = 0.3 ft.

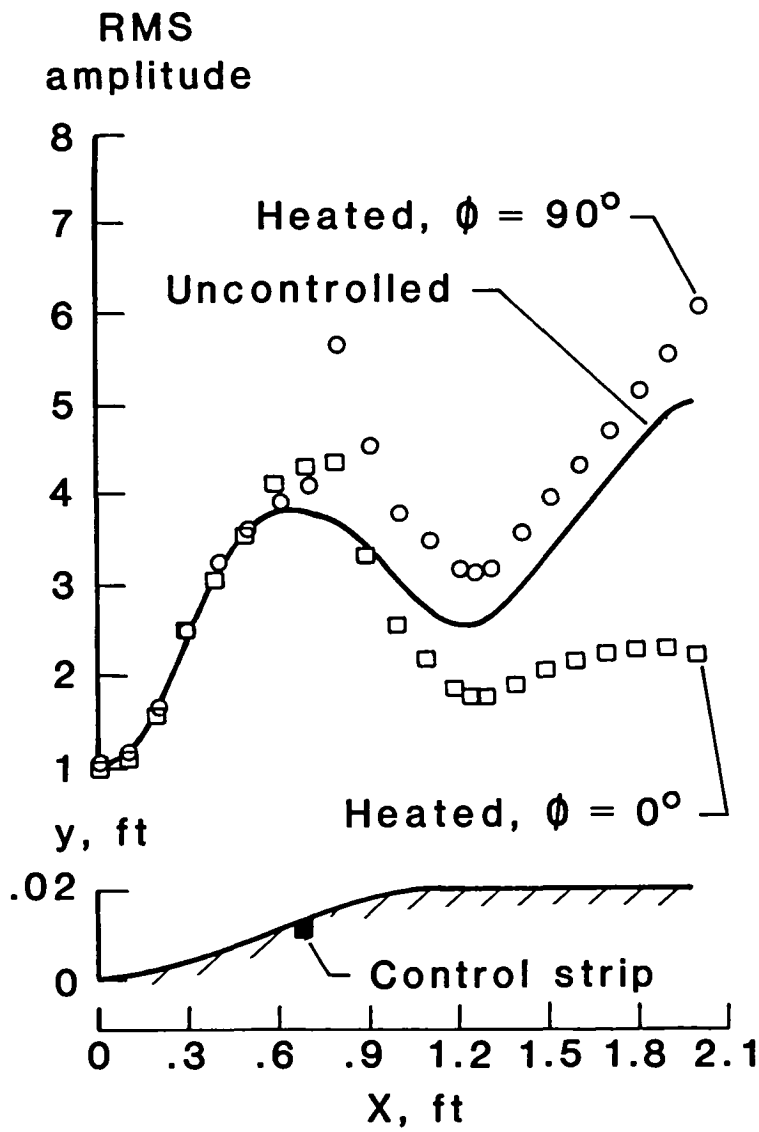

Fig. 6. Effectiveness of Active Control by Heating, Control Strip at x = 0.7 ft.

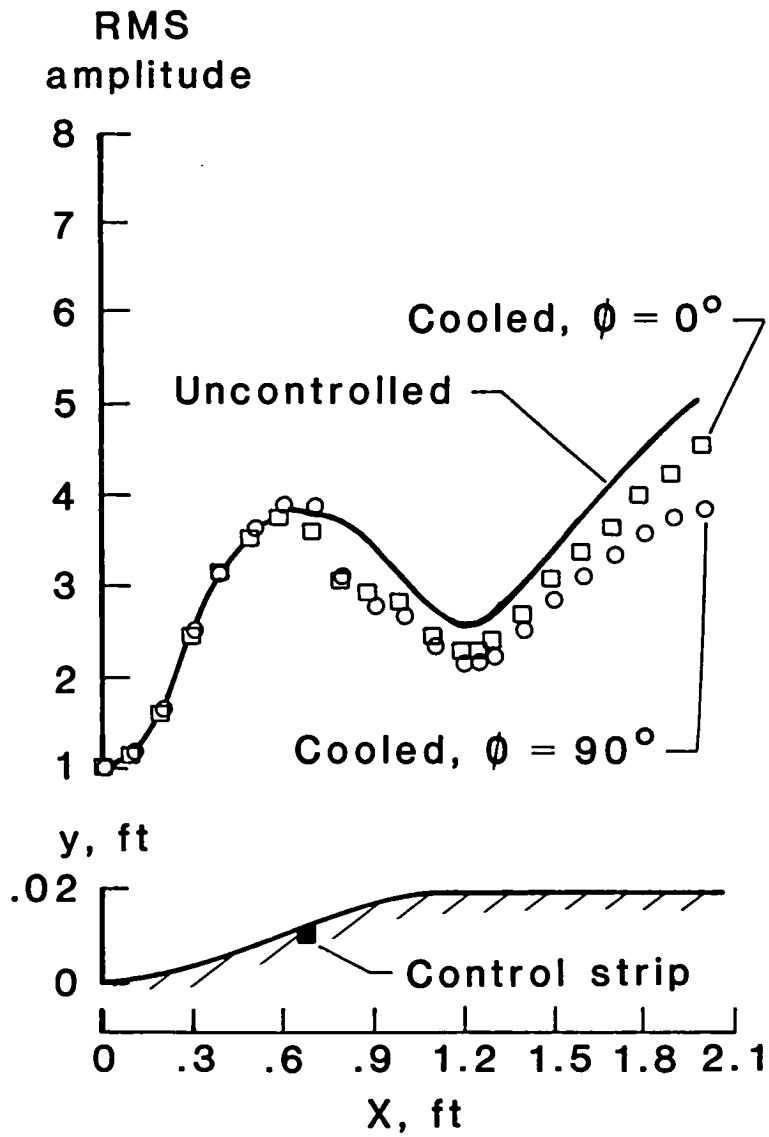

Fig. 7. Effectiveness of Active Control by Cooling, Control Strip at x = 0.7 ft.

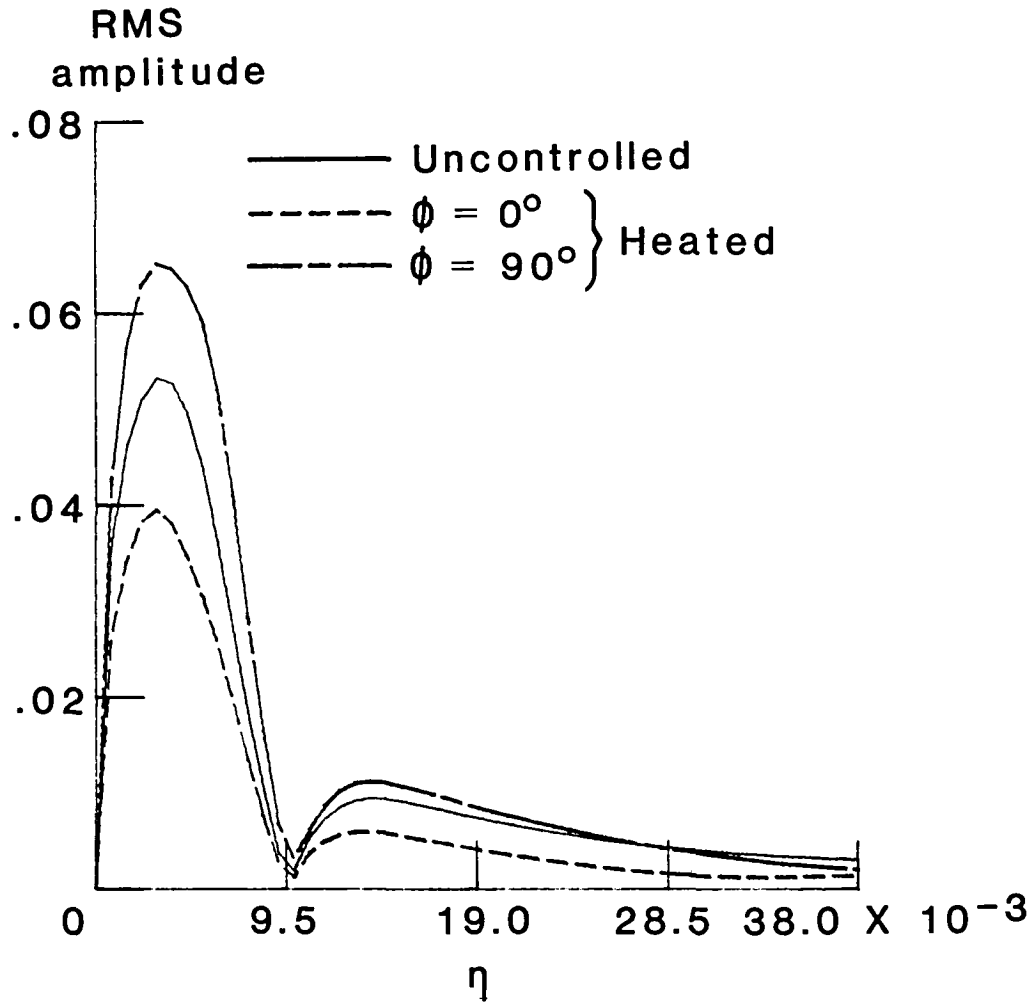

Fig. 8. Comparison of RMS Amplitude Across the Boundary Layer at x = 0.5 ft. with Control at x = 0.3 ft.

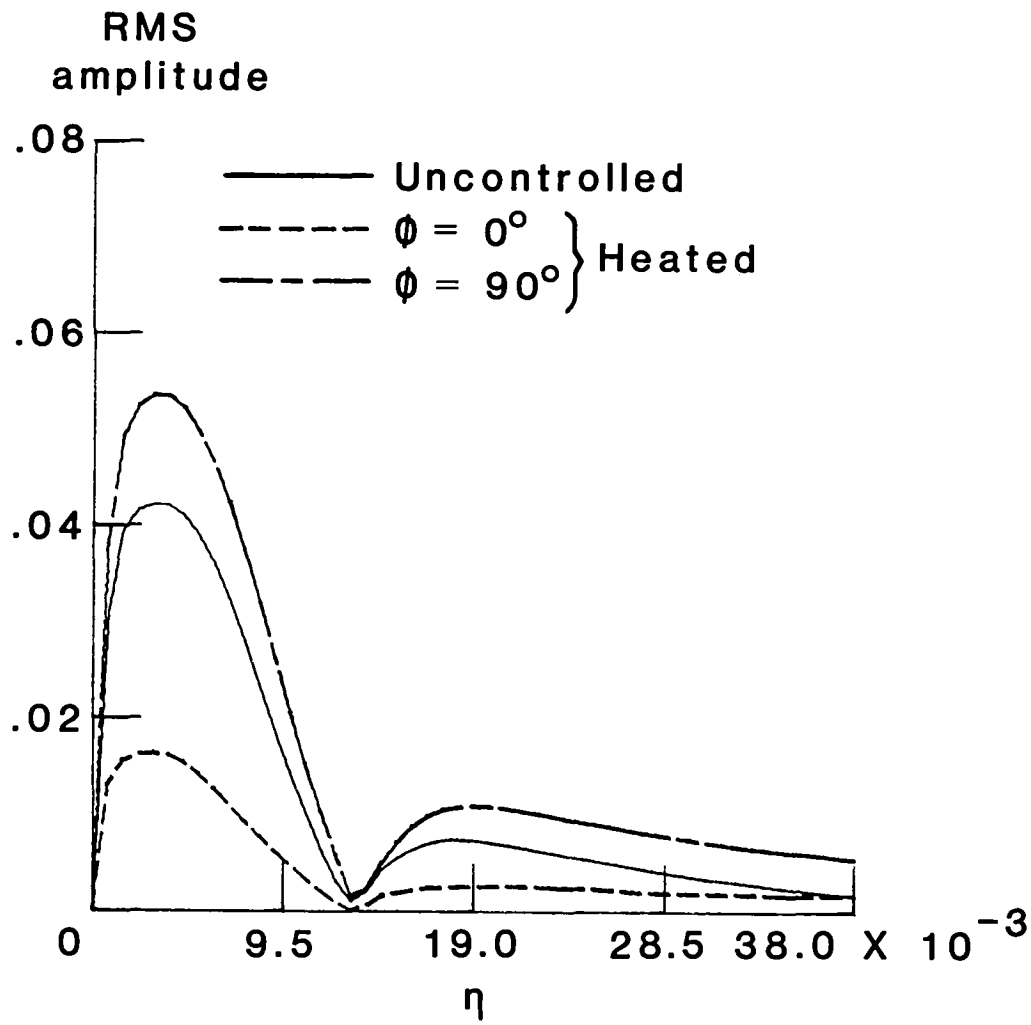

Fig. 9. Comparison of RMS Amplitude Across the Boundary Layer at x = 1.5 ft. with Control at x = 0.3 ft.

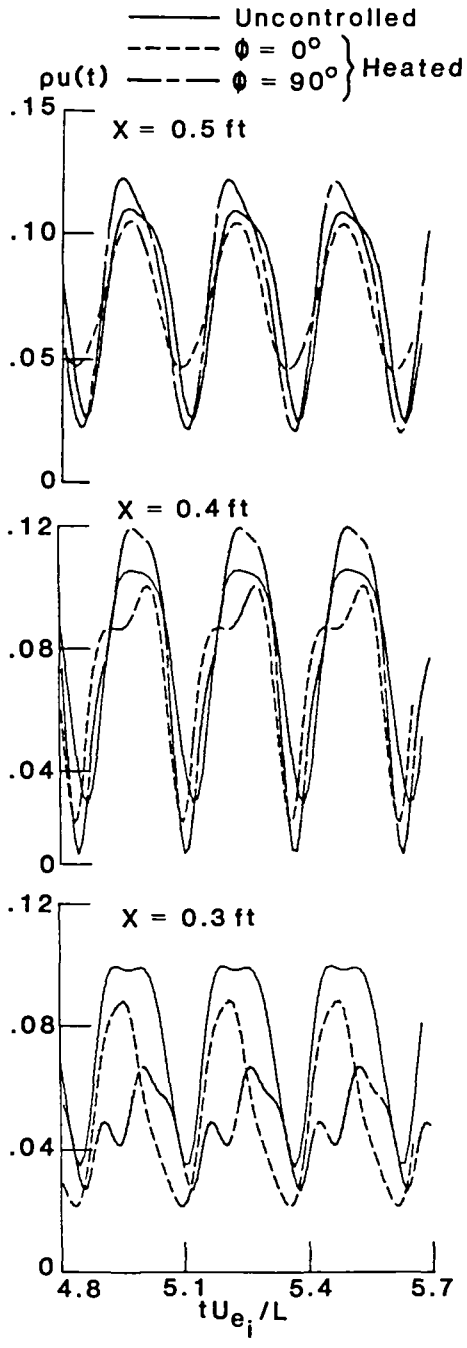

Fig. 10 Comparison of $\rho u(t)$ Between Controlled and Uncontrolled Cases for a Location Close to the Wall ($\eta = 0.55 \times 10^{-3}$).

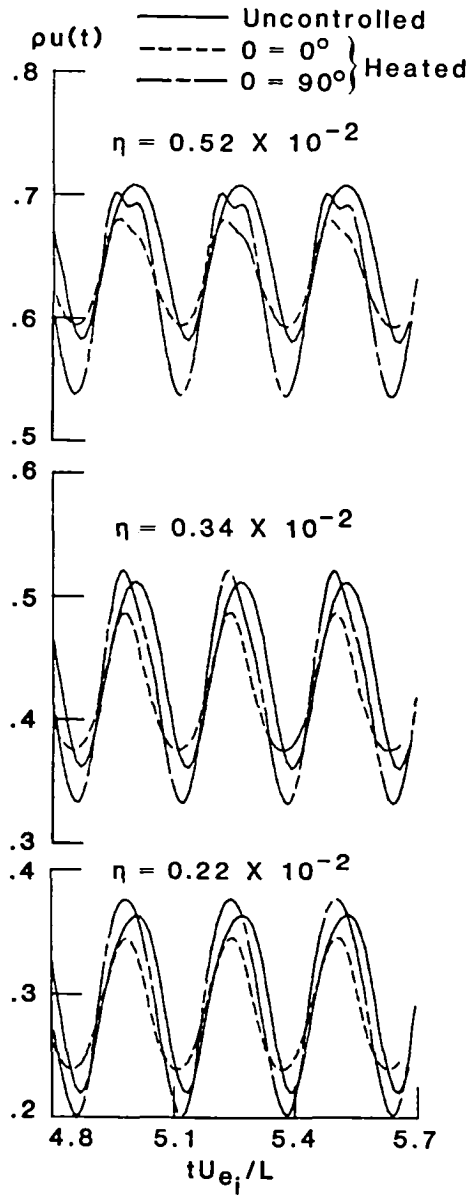

Fig. 11. Comparison of ρu(t) Across the Boundary Layer Between Controlled and Uncontrolled Cases at x = 0.5 ft.

1. Report No. NASA CR-178018 ICASE Report No. 85-52	2. Government Accession No.	3. Recipient's Catalog No.
4. Title and Subtitle ACTIVE CONTROL OF COMPRESSIBLE FLOWS ON A CURVED SURFACE		5. Report Date November 1985 6. Performing Organization Code
7. Author(s) Maestrello, Lucio, Paresh Parikh, Alvin Bayliss, and Eli Turkel		8. Performing Organization Report No. 85-52 10. Work Unit No.
9. Performing Organization Name and Address Institute for Computer Applications in Science and Engineering Mail Stop 132C, NASA Langley Research Center Hampton, VA 23665-5225		11. Contract or Grant No. NAS1-17070; NAS1-18107 13. Type of Report and Period Covered Contractor Report
12. Sponsoring Agency Name and Address National Aeronautics and Space Administration Washington, D.C. 20546		14. Sponsoring Agency Code 505-31-83-01

15. Supplementary Notes

Langley Technical Monitor:
J. C. South Jr.
Final Report

Submitted to SAE Aerospace Technology Conference

16. Abstract

We consider the effect of localized, time-periodic surface heating and cooling over a curved surface. This is a mechanism for the active control of unstable disturbances by phase cancellation and reinforcement. It is shown that the pressure gradient induced by the curvature significantly enhances the effectiveness of this form of active control. In particular, by appropriate choice of phase, active surface heating can completely stabilize an unstable wave.

17. Key Words (Suggested by Author(s))	18. Distribution Statement
fluid dynamics, fourth-order finite differences	34 - Fluid Mechanics & Heat Transfer 64 - Numerical Analysis Unclassified - Unlimited

19. Security Classif. (of this report)	20. Security Classif. (of this page)	21. No. of Pages	22. Price
Unclassified	Unclassified	28	A03

For sale by the National Technical Information Service, Springfield, Virginia 22161